

THEORETICAL AND NUMERICAL ASPECTS OF THE INTERFACIAL COUPLING : THE SCALAR RIEMANN PROBLEM AND AN APPLICATION TO MULTIPHASE FLOWS

CHRISTOPHE CHALONS

CEA-Saclay
DEN/DANS/DM2S/SFME/LETR
F-91191 Gif-sur-Yvette, France

ABSTRACT. This paper is devoted to the study of the one dimensional interfacial coupling of two PDE systems at a given fixed interface, say $x = 0$. Each system is posed on a half-space, namely $x < 0$ and $x > 0$. As an interfacial model, a coupling condition whose objective is to enforce the continuity (in a weak sense) of a prescribed variable is generally imposed at $x = 0$.

We first focus on the coupling of two scalar conservation laws and state an existence result for the coupled Riemann problem. Numerical experiments are also proposed. We then consider, both from a theoretical and a numerical point of view, the coupling of two-phase flow models namely a drift-flux model and a two-fluid model. In particular, the link between both models will be addressed using asymptotic expansions.

1. Introduction. This paper follows a presentation given by the author at the conference *New Trends in Model Coupling. Theory, Numerics and Applications* held in Paris (France) in September 2009. It aimed at briefly presenting some results obtained recently in the context of a collaboration between the Laboratoire Jacques-Louis Lions (<http://www.ann.jussieu.fr>) and the CEA-Saclay (<http://www-centre-saclay.cea.fr/index.php/en>) on the coupling problem of nonlinear systems of partial differential equations. The following persons have taken (or took) part in this collaboration : A. Ambroso, B. Boutin, C. Chalons, F. Coquel, T. Galié, E. Godlewski, F. Lagoutière, P.-A. Raviart, J. Segré, Nicolas Seguin. We refer the reader to <http://www.ann.jussieu.fr/groupes/cea> for more details. We have been more precisely interested in the development of theoretically grounded numerical tools for the coupling of two-phase flow models. With this in mind, we have studied a wide hierarchy of models : scalar conservation laws, gas dynamics equations, homogeneous models for two-phase flows, drift-flux models and bifluid systems. The industrial motivation is concerned with the simulation of nuclear reactors when several thermohydraulic codes are used. In these codes, multiple modelling scales are applied to describe the flow. For instance, different models can be used for each reactor component to take into account its specific behavior, or small scale models can be used, locally, to obtain a better resolution. When these models are put side to side, we face the problem of coupling. There is therefore

2000 *Mathematics Subject Classification.* 35L50, 35L60, 35L65, 65M12, 65M30, 76M12, 76T10.

Key words and phrases. Coupling problem, Discontinuous flux function, Riemann problem, Two-phase flow models, Drift flux models.

a need to identify the nature of the information to be transmitted at a coupling interface in order to obtain a coherent description of the whole operating device.

The first part of the paper is devoted to the coupling of two scalar conservation laws. We first explain how the coupling problem is set from a mathematical point of view by precisizing the coupling condition we impose at the coupling interface. We then state an existence result for the Riemann problem and highlight some interesting features like existence and non uniqueness of both continuous and discontinuous (at the coupling interface) solutions. The numerical standpoint is also investigated.

The second part of the paper is concerned with the coupling of two two-phase flow models, namely a two-fluid two-pressure model and a drift-flux model. After a brief presentation of the dimensionless forms of these models, we first state a proximity result of their solutions to each other. This statement relies on a Chapman-Enskog asymptotic analysis with respect to a small parameter ϵ . This parameter naturally comes out when considering real-like applications and expresses, roughly speaking, that the various relaxation times involved in the (two-pressure) model are much smaller than the time scale of interest. We then briefly describe the proposed numerical coupling procedure and assess it on a classical vertical bubbly column test case. A particular attention is paid to the numerical validity of the above mentioned proximity result in the asymptotic regime $\epsilon \rightarrow 0$.

The two parts of the paper are independent.

This work was partially supported by the NEPTUNE project [18], funded by CEA, EDF, IRSN and AREVA-NP.

2. Interfacial coupling of two scalar conservation laws. In this section, we focus on the coupling of two *scalar* conservation laws at a fixed interface, say for instance $x = 0$. Each equation is associated with its own smooth flux function and is posed on a half-space, namely $x < 0$ and $x > 0$. More precisely, the problem writes as follows :

$$\partial_t u + \partial_x f_L(u) = 0, \quad x < 0, \quad t > 0 \quad (1)$$

$$\partial_t u + \partial_x f_R(u) = 0, \quad x > 0, \quad t > 0 \quad (2)$$

where $f_\alpha : \mathbb{R} \rightarrow \mathbb{R}$, $\alpha = L, R$, are two given C^1 functions. Note that it will be implicitly assumed throughout the paper that the flux functions f_α have at most a finite number of changes of convexity, which is often (is not always) the case for practical applications. Given $u_0 : \mathbb{R} \rightarrow \mathbb{R}$, we impose the initial condition

$$u(x, 0) = u_0(x), \quad x \in \mathbb{R}. \quad (3)$$

At this stage, the coupling condition at point $x = 0$ remains to be precisized. Without further details, we assume here that it is physically relevant to impose the continuity of a given quantity $v_\alpha = v_\alpha(u)$ at the coupling interface, that is to look for a solution $u : (x, t) \rightarrow u(x, t) \in \mathbb{R}$ such that

$$v_L(u(0_-, t)) = v_R(u(0_+, t)), \quad t > 0. \quad (4)$$

This continuity constraint will be understood in a weak sense hereafter.

2.1. Towards a weakened coupling condition. In order to illustrate the need for a weakened coupling condition instead of (4), let us temporarily concentrate on the simplest case $v_\alpha(u) = u$, $\alpha = L, R$, so that (4) reads

$$u(0_-, t) = u(0_+, t), \quad t > 0. \quad (5)$$

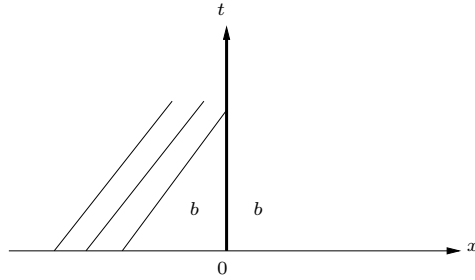


FIGURE 1. Information travelling with positive speed in a boundary value problem set in $x < 0$

Then, the coupling problem (1)-(2)-(4) can be understood as two boundary value problems, namely a “right” boundary value problem for the “left” system (1) and a “left” boundary value problem for the “right” system (2) :

$$\begin{cases} \partial_t u + \partial_x f_L(u) = 0, & x < 0, t > 0 \\ u(0_-, t) = b_L(t), & t > 0 \end{cases} \quad \text{and} \quad \begin{cases} \partial_t u + \partial_x f_R(u) = 0, & x > 0, t > 0 \\ u(0_+, t) = b_R(t), & t > 0 \end{cases}$$

with $b_L(t) = u(0_+, t)$ and $b_R(t) = u(0_-, t)$. Now in this context, it is well-known that given u_0, f, b and the following initial boundary value problem set for instance in $x < 0$,

$$\begin{cases} \partial_t u + \partial_x f(u) = 0, & x < 0, t > 0 \\ u(0_-, t) = b, & t > 0 \\ u(x, 0) = u_0(x), & x < 0 \end{cases} \tag{6}$$

one cannot always impose $u(0_-, t) = b, t > 0$ in the strong sense since information may travel with positive speed depending on the flux function f , see Figure 1. The boundary condition $u(0_-, t) = b, t > 0$ must therefore be understood in a weak sense. Following LeFloch and Dubois [13] and denoting $w(\frac{x}{t}; u_g, u_d)$ the self-similar solution of the Riemann problem

$$\begin{cases} \partial_t u + \partial_x f(u) = 0, & \underline{x} \in \mathbb{R}, t > 0 \\ u(x, 0) = \begin{cases} u_g, & x < 0 \\ u_d, & x > 0 \end{cases} \end{cases}$$

we propose to replace $u(0_-, t) = b, t > 0$ with

$$u(0_-, t) \in \mathcal{O}(b), t > 0, \tag{7}$$

the set $\mathcal{O}(b)$ being defined by

$$\mathcal{O}(b) = \{w(0_-; u, b); u \in \mathbb{R}\}.$$

The boundary value b obviously belongs to this set of admissible values since $w(0_-; b, b) = b$. More generally, (7) means that the left trace $u(0_-, t)$ of the solution must coincide with the left trace (at point $x = 0$) of a Riemann solution for which the right state u_d of the initial condition is b . In other words, the Riemann solution $w(\cdot; u_g, u_d)$ for which the left and right states u_g and u_d are respectively $u(0_-, t)$ and b must only have waves propagating with a non negative speed, see Figure 2.

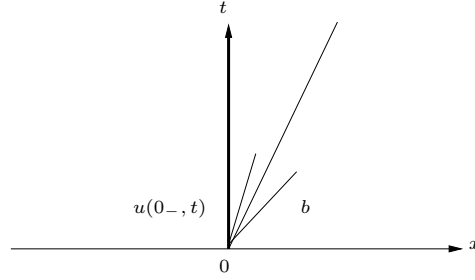


FIGURE 2. An example of admissible left trace $u(0_-, t)$: the Riemann solution $w(\frac{x}{t}; u(0_-, t), b)$ has non negative speeds only

Consider now the more general initial boundary value problem

$$\begin{cases} \partial_t u + \partial_x f(u) = 0, & x < 0, t > 0 \\ v(0_-, t) := \theta^{-1}(u(0_-, t)) = b, & t > 0 \\ u(x, 0) = u_0(x), & x < 0 \end{cases} \quad (8)$$

for a given invertible function θ^{-1} . Setting

$$z\left(\frac{x}{t}; v_g, v_d\right) = \theta^{-1}\left(w\left(\frac{x}{t}; \theta(v_g), \theta(v_d)\right)\right)$$

the boundary condition $v(0_-, t) := \theta^{-1}(u(0_-, t)) = b$ is naturally replaced with

$$v(0_-, t) \in \tilde{\mathcal{O}}(b), \quad t > 0, \quad (9)$$

the set $\tilde{\mathcal{O}}(b)$ being defined by

$$\tilde{\mathcal{O}}(b) = \{z(0_-; v, b); v \in \mathbb{R}\}.$$

Remark 1. The invertibility assumption on θ^{-1} is necessary for $z(\cdot, \cdot, \cdot)$ and then $\tilde{\mathcal{O}}(b)$ to be well-defined. This assumption is thus necessary as soon as we deal with solutions of the initial boundary value problem (8) such that the continuity condition $v(0_-, t) := \theta^{-1}(u(0_-, t)) = b$ is not satisfied in the strong sense.

2.2. The mathematical formulation of the coupling problem. It is now clear that the coupling condition (4) must be understood in a weak sense. Let us assume that $v_\alpha(u) = \theta_\alpha^{-1}(u)$, $\alpha = L, R$ for two given invertible functions θ_α^{-1} , $\alpha = L, R$. We set

$$v(x, t) = \begin{cases} \theta_L^{-1}(u(x, t)), & x < 0 \\ \theta_R^{-1}(u(x, t)), & x > 0. \end{cases} \quad (10)$$

Along the lines of the previous subsection and following [13], [16] and [17], (4) is given the following weak sense :

$$\begin{cases} v(0_-, t) \in \tilde{\mathcal{O}}_L(v(0_+, t)) \\ v(0_+, t) \in \tilde{\mathcal{O}}_R(v(0_-, t)), \end{cases} \quad (11)$$

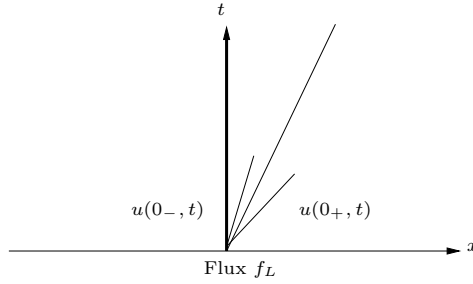


FIGURE 3. An example of admissible left trace $u(0_-, t)$: the Riemann solution $w_L(\frac{x}{t}; u(0_-, t), u(0_+, t))$ has non negative speeds only

where the sets $\tilde{\mathcal{O}}_L(v_d)$ and $\tilde{\mathcal{O}}_R(v_g)$ are naturally defined as follows. Denoting by $w_\alpha(\frac{x}{t}; u_g, u_d)$ the self-similar solution of the Riemann problem

$$\begin{cases} \partial_t u + \partial_x f_\alpha(u) = 0, \quad \underline{x \in \mathbb{R}}, \quad t > 0 \\ u(x, 0) = \begin{cases} u_g, & x < 0 \\ u_d, & x > 0 \end{cases} \end{cases}$$

and setting

$$z_\alpha(\frac{x}{t}; v_g, v_d) = \theta_\alpha^{-1}(w_\alpha(\frac{x}{t}; \theta_\alpha(v_g), \theta_\alpha(v_d)))$$

we have

$$\begin{cases} \tilde{\mathcal{O}}_L(v_d) = \{z_L(0_-; v, v_d); v \in \mathbb{R}\} \\ \tilde{\mathcal{O}}_R(v_g) = \{z_R(0_+; v_g, v); v \in \mathbb{R}\}. \end{cases}$$

Focusing on the particular case $\theta_\alpha^{-1}(u) = u$, $\alpha = L, R$, the weakened coupling condition (11) means that the left trace $u(0_-, t)$ (respectively the right trace $u(0_+, t)$) of the solution of the coupled problem must coincide with the left trace (resp. the right trace) of a Riemann solution associated with the flux f_L (resp. f_R) and for which the right state u_d (resp. the left state u_g) of the initial condition is $u(0_+, t)$ (resp. $u(0_-, t)$). In other words, the Riemann solution $w_\alpha(\cdot; u(0_-, t), u(0_+, t))$ must only have waves propagating with a non negative (respectively non positive) speed for $\alpha = L$ (resp. $\alpha = R$), see Figures 3 and 4.

Remark 2. Here again, the invertibility assumptions on θ_α^{-1} are necessary for the sets $\tilde{\mathcal{O}}_\alpha(v)$, $\alpha = L, R$ to be well-defined. This assumption is thus necessary as soon as we deal with solutions of the coupling problem (1)-(2)-(11) such that $v(0_-, t) \neq v(0_+, t)$. In this case, the continuity constraint $v(0_-, t) = v(0_+, t)$ is satisfied in a weak sense only.

3. An existence result for the coupled Riemann problem. In this section, we consider the Riemann problem associated with the coupled problem under consideration, meaning that we look for a self-similar solution of (1)-(2), supplemented with the weakened coupling condition (11) and the initial condition

$$u(x, 0) = \begin{cases} u_g, & x < 0 \\ u_d, & x > 0 \end{cases}$$

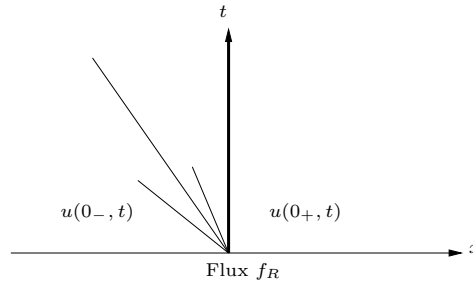


FIGURE 4. An example of admissible right trace $u(0_+, t)$: the Riemann solution $w_R(\frac{x}{t}; u(0_-, t), u(0_+, t))$ has non positive speeds only

for two given initial states u_g and u_d . For convenience, we assume that both functions θ_L and θ_R are strictly increasing and map \mathbb{R} onto itself.

In [10], we proved the following existence result.

Theorem 3.1. ([10]) *Assume that the flux functions f_L and f_R are C^1 functions with at most a finite number of convexity changes. Then the coupled Riemann problem has at least one self-similar solution.*

Instead of proving this theorem, which would be too long for the present limited in length paper, we propose to illustrate it on particular flux functions.

Let us first briefly give some comments. Firstly, the solution to the coupled Riemann problem can be either continuous or discontinuous in the v -variable at the coupling interface. In the former case, the coupling condition (4) is satisfied in the classical sense, while in the latter one, this continuity constraint is satisfied in the weak sense (11) only. Secondly, it is worth noticing that the solution to the Riemann problem exists but is not necessarily unique. In fact, in some particular situations, continuous and discontinuous solutions at the coupling interface (and in the v -variable) may co-exist, the latter one being not necessarily unique. At last, note that even a 1-parameter family of continuous solutions at the coupling interface may exist for the same Riemann initial data.

3.1. Some particular configurations. In this section, we set $v_L(u) = v_R(u) = u$.

3.1.1. The functions f_L and f_R are strictly decreasing. In this case, information propagates with negative speed so that the right trace of the solution $u(0_+, t)$ at the coupling interface necessarily equals u_d . More precisely, we have

$$u(x, t) = u_d, x > 0.$$

As far as the left trace $u(0_-, t)$ is concerned, the coupling condition $u(0_-, t) \in \mathcal{O}_L(u_d)$ imposes that the Riemann solution $w_L(\cdot; u(0_-, t), u_d)$ has only waves propagating with non negative speeds. Since f_L is strictly decreasing, this is not possible except if the waves are trivial which means that $u(0_-, t) = u_d$. The Riemann solution to the coupled Riemann problem is therefore continuous at the coupling interface and equals u_d :

$$u(0_-, t) = u(0_+, t) = u_d,$$

see Figure 5.

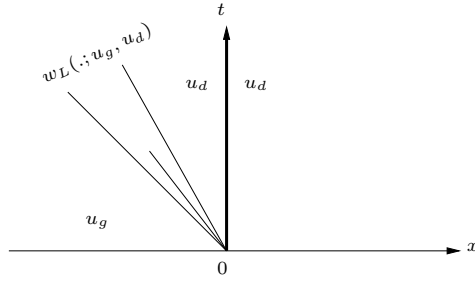


FIGURE 5. The functions f_L and f_R are strictly decreasing

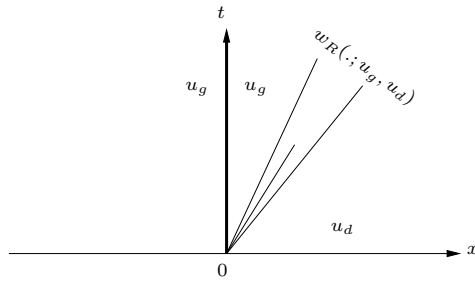


FIGURE 6. The functions f_L and f_R are strictly increasing

3.1.2. *The functions f_L and f_R are strictly increasing.* This case is similar to the previous one. Here, information propagates with positive speed so that the left trace of the solution $u(0_-, t)$ at the coupling interface necessarily equals u_g . More precisely,

$$u(x, t) = u_g, x < 0.$$

Regarding the right trace $u(0_+, t)$, the coupling condition $u(0_+, t) \in \mathcal{O}_R(u_g)$ imposes that the Riemann solution $w_R(\cdot; u_g, u(0_+, t))$ has only waves propagating with non positive speeds. Since f_R is strictly increasing, this is not possible except if the waves are trivial meaning that $u(0_+, t) = u_g$. The Riemann solution is thus continuous and equals u_g at the coupling interface :

$$u(0_-, t) = u(0_+, t) = u_g,$$

see Figure 6.

3.1.3. *The function f_L is strictly increasing and the function f_R is strictly decreasing.* Here, information propagates with positive speed in the domain $\{x < 0\}$ and with negative speed in the domain $\{x > 0\}$ so that we necessarily have $u(0_-, t) = u_g$ and $u(0_+, t) = u_d$. Let us now concentrate on the coupling condition which writes here $u_g \in \mathcal{O}_L(u_d)$ and $u_d \in \mathcal{O}_R(u_g)$. The Riemann solution $w_L(\cdot; u_g, u_d)$ (respectively $w_R(\cdot; u_g, u_d)$) must only have waves propagating with non negative (resp. non positive) speeds. This is obviously true since f_L (resp. f_R) is strictly increasing (resp. strictly decreasing). The Riemann solution to the coupled Riemann problem is thus a stationary discontinuity, see Figure 7.

3.1.4. *The function f_L is strictly decreasing and the function f_R is strictly increasing.* Here, information propagates with negative speed in the domain $\{x < 0\}$ and

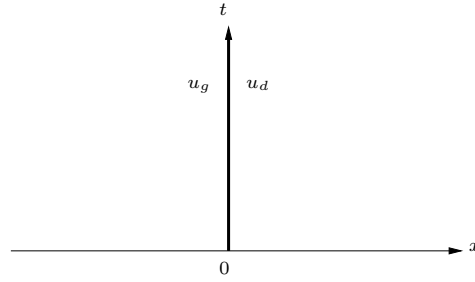


FIGURE 7. The function f_L is strictly increasing and the function f_R is strictly decreasing

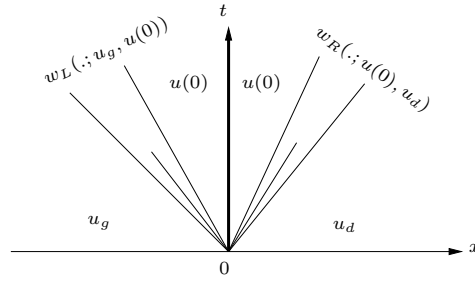


FIGURE 8. The function f_L is strictly decreasing and the function f_R is strictly increasing

with positive speed in the domain $\{x > 0\}$ so that the values $u(0_-, t)$ and $u(0_+, t)$ cannot be defined from the initial data. Regarding the coupling condition, the Riemann solution $w_L(\cdot; u(0_-, t), u(0_+, t))$ (respectively $w_R(\cdot; u(0_-, t), u(0_+, t))$) must only have waves propagating with non negative (resp. non positive) speeds. This is not possible since f_L (resp. f_R) is strictly decreasing (resp. strictly increasing), except if $u(0_-, t) = u(0_+, t)$. The solutions to the coupled Riemann problem are thus u -continuous at the coupling interface and form a one-parameter family depending on the parameter $u(0) := u(0_-, t) = u(0_+, t) \in \mathbb{R}$, see Figure 8.

4. Numerical experiments. The aim of this section is to illustrate the theoretical statements of the previous section from a numerical point of view. Note from now on that the numerical results of this section, and additional ones as well, can be found in [10]. Here, two particular configurations will be considered. The first one corresponds to the case of two strictly monotone flux functions f_L and f_R . The second one corresponds to a situation leading to two admissible discontinuous solutions at the coupling interface. Interestingly, we will observe that different numerical schemes may capture different solutions.

Let us begin with a brief description of the numerical scheme.

4.1. Numerical scheme. We propose a finite volume method for the discretization of both systems (1) and (2). Let Δx and Δt denote the uniform steps for space and time, and let $\mathcal{C}_{j+1/2}$ be the cells defined by $\mathcal{C}_{j+1/2} = (x_j, x_{j+1})$ with $x_j = j\Delta x$ and whose centers are $x_{j+1/2} = (j + 1/2)\Delta x$ for all $j \in \mathbb{Z}$. We set $\lambda = \Delta t/\Delta x$ and $t_n = n\Delta t$ for $n \in \mathbb{N}$. The approximate solution is assumed to be piecewise constant

on each cell $\mathcal{C}_{j+1/2}$ and at each time t^n and the corresponding value is denoted $u_{j+1/2}^n$. As is usual, we first set

$$u_{j+1/2}^0 = \frac{1}{\Delta x} \int_{\mathcal{C}_{j+1/2}} u_0(x) dx, \quad j \in \mathbb{Z},$$

where u_0 denotes a given initial condition for the coupling problem.

Then, let G_α , $\alpha = L, R$ be two two-point numerical flux functions such that $G_\alpha(u, u) = f_\alpha(u)$, $\alpha = L, R$ (consistency). We propose the following update formula for $u_{j+1/2}^{n+1}$:

$$\begin{aligned} u_{j-1/2}^{n+1} &= u_{j-1/2}^n - \lambda(G_{L,j}^n - G_{L,j-1}^n), & j \leq 0, \quad n \geq 0, \\ u_{j+1/2}^{n+1} &= u_{j+1/2}^n - \lambda(G_{R,j+1}^n - G_{R,j}^n), & j \geq 0, \quad n \geq 0, \end{aligned} \tag{12}$$

with $G_{\alpha,j}^n = G_\alpha(u_{j-1/2}^n, u_{j+1/2}^n)$ for $j \neq 0$. Said differently, the scheme is a classical finite volume scheme “far away” from the interface, while both fluxes $G_{L,0}^n$ and $G_{R,0}^n$ remain to be precised in order to define the numerical coupling procedure. Following the previous works [16], [17] (see also [1], [2], [3], [4], [5], [6]), we set in [10]

$$\begin{aligned} G_{L,0}^n &= G_L(u_{-1/2}^n, \theta_L(v_{1/2}^n)), \\ G_{R,0}^n &= G_R(\theta_R(v_{-1/2}^n), u_{1/2}^n), \end{aligned} \tag{13}$$

where ghost states $v_{\pm 1/2}^n$ are obtained as

$$\begin{aligned} v_{-1/2}^n &= \theta_L^{-1}(u_{-1/2}^n), \\ v_{1/2}^n &= \theta_R^{-1}(u_{1/2}^n). \end{aligned} \tag{14}$$

For convenience , we will restrict ourselves to the simple case $\theta_L = \theta_R = id$, so that the ghost states at the interface are simply

$$\begin{aligned} v_{-1/2}^n &= u_{-1/2}^n, \\ v_{1/2}^n &= u_{1/2}^n. \end{aligned} \tag{15}$$

At last and as far as the numerical flux functions G_α , $\alpha = L, R$ are concerned, we will consider the celebrated Godunov scheme :

$$G_\alpha(u, v) = \begin{cases} \min_{w \in [u,v]} f_\alpha(w), & u \leq v, \\ \max_{w \in [v,u]} f_\alpha(w), & v < u, \end{cases} \tag{16}$$

and a relaxation scheme (see for instance [21]) defined by :

$$G_\alpha(u, v) = \frac{1}{2}(f_\alpha(u) + f_\alpha(v)) + \frac{a(u, v)}{2}(u - v) \quad \text{with} \quad a(u, v) = \max_{[\min(u,v), \max(u,v)]} |f'|. \tag{17}$$

4.2. Numerical results. Let us now present the test cases and the numerical results. As Riemann initial data, we take

$$u_0(x) = \begin{cases} u_g & \text{if } x < 0, \\ u_d & \text{if } x > 0. \end{cases}$$

Test 1. The case of strictly monotone flux functions.

We choose $u_g = -2$ and $u_d = 2$ and we consider the following cases :

- (a) $f_L(u) = -u$ and $f_R(u) = -2u$: the unique solution is continuous at the coupling interface.
- (b) $f_L(u) = u$ and $f_R(u) = 2u$: the unique solution is continuous at the coupling interface.

- (c) $f_L(u) = u$ and $f_R(u) = -2u$: there is no continuous solution but a unique discontinuous solution.
- (d) $f_L(u) = -u$ and $f_R(u) = 2u$: there is no discontinuous solution and a continuum of continuous solutions.

Numerical results, obtained for both relaxation and Godunov approaches, are presented on Fig. 9. These results are in agreement with the above theoretical results. Note that in the last case, a one-parameter family of solutions does exist but both numerical schemes capture the same continuous solution.

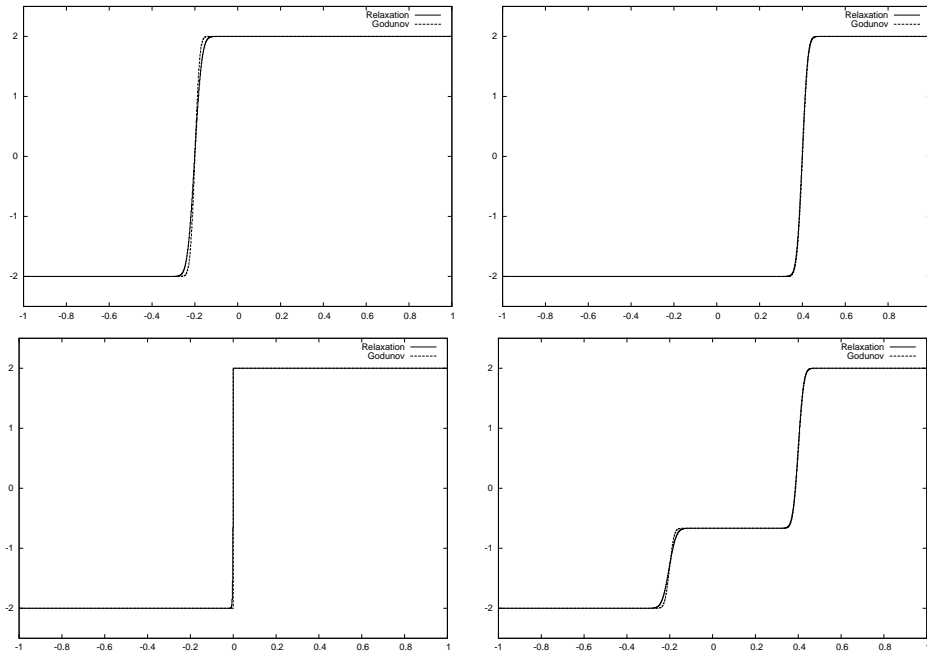


FIGURE 9. Monotone fluxes. Top : Left (a), Right (b). Bottom : Left (c), Right (d). 1000-point mesh. $t = 0.2$. $u_g = -2$, $u_d = 2$.

Test 3. A particular configuration where two discontinuous solutions are admissible.

The flux functions f_L and f_R are defined from the derivatives f'_L and f'_R given by

$$f'_L(u) = (u + 1)\left(u + \frac{1}{10}\right)(u - 1),$$

$$f'_R(u) = -\left(u + \frac{1}{2}\right)\left(u - \frac{2}{5}\right)\left(u - \frac{3}{2}\right).$$

The Riemann initial data is such that $u_g = -1.25$ and $u_d = 1.75$. It can be proved, see [10], that the Riemann problem admits two discontinuous solutions. Numerical solutions are presented on Fig. 10. We observe that the Godunov scheme and the relaxation scheme do not capture the same solution.

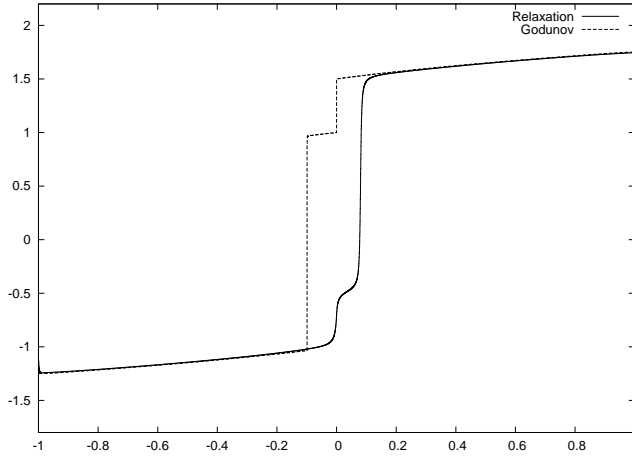


FIGURE 10. Multiple discontinuous solutions. 10000-point mesh.
 $u_L = -1.25, u_R = 1.75, t = 1.5$

5. Application to multiphase flows. In this part, we are now interested in the coupling of two-phase flow models, namely a two-pressure model and a drift-flux model. This coupling problem is motivated by real applications in the nuclear domain and more precisely by the simulation of the flows in the core or steam generator of a nuclear reactor, say for instance a Pressurized or Boiling Water Reactor. In this context, liquid-vapor water flows are naturally present and may be described by different sets of equations depending on their specificities. One assumes here that both the two-pressure and drift-flux systems are relevant, and thus investigate their coupling. Let us begin with a brief description of the models, focusing ourselves on the barotropic case.

The two-fluid two-pressure model. The two-pressure model we consider is made of five equations associated with the following five unknowns : the void fraction α_1 of the phase 1 (the void fraction of the phase 2 is given by $\alpha_2 = 1 - \alpha_1$), the densities ρ_1 and ρ_2 of the two phases, and the corresponding velocities u_1 and u_2 . We set $\mathbf{u} = (\alpha_1, \alpha_1\rho_1, \alpha_2\rho_2, \alpha_1\rho_1u_1, \alpha_2\rho_2u_2)$.

The governing equations, written in dimensionless form, are given as follows :

$$\begin{cases} \partial_t \alpha_1 + u_I \partial_x \alpha_1 = \Theta(\mathbf{u})(p_1 - p_2) \\ \partial_t \alpha_1 \rho_1 + \partial_x \alpha_1 \rho_1 u_1 = 0 \\ \partial_t \alpha_2 \rho_2 + \partial_x \alpha_2 \rho_2 u_2 = 0 \\ \partial_t (\alpha_1 \rho_1 u_1) + \partial_x (\alpha_1 \rho_1 u_1^2 + \alpha_1 p_1(\rho_1)) - p_I \partial_x \alpha_1 = \\ \alpha_1 \rho_1 f_1(\mathbf{u}) + \Lambda(\mathbf{u}) |u_2 - u_1| (u_2 - u_1) \\ \partial_t (\alpha_2 \rho_2 u_2) + \partial_x (\alpha_2 \rho_2 u_2^2 + \alpha_2 p_2(\rho_2)) + p_I \partial_x \alpha_1 = \\ \alpha_2 \rho_2 f_2(\mathbf{u}) + \Lambda(\mathbf{u}) |u_1 - u_2| (u_1 - u_2) \end{cases} \quad (18)$$

We first observe that the void fraction α_1 evolves according to a transport equation with (interfacial) velocity u_I and supplemented with a pressure relaxation term. The relaxation coefficient is given by $1/\Theta(\mathbf{u})$ and the corresponding equilibrium is given by an equality of the barotropic pressures of the two phases, that is $p_1(\rho_1) = p_2(\rho_2)$. Then we have two classical mass conservation equations for each phase, and at last two evolution equations for the momentum $\alpha_1 \rho_1 u_1$ and $\alpha_2 \rho_2 u_2$. In these equations,

we first emphasize in the left-hand side the presence of two nonconservative products $p_I \partial_x \alpha_1$ where p_I denotes an interfacial pressure, and in the right-hand side the presence of a velocity relaxation term to the equilibrium $u_1 = u_2$. The relaxation coefficient is given by $1/\Lambda(\mathbf{u})$. The functions $f_1(\mathbf{u})$ and $f_2(\mathbf{u})$ correspond to the external forces and will be set to the gravity constant $-g$ in the following.

We will assume throughout this section that the pressure and velocity relaxation coefficients have the following forms :

$$\Lambda(\mathbf{u}) = \frac{\lambda(\mathbf{u})}{\epsilon^2}, \quad \Theta(\mathbf{u}) = \frac{\theta(\mathbf{u})}{\epsilon^2}$$

where importantly, $\lambda(\mathbf{u})$ and $\theta(\mathbf{u})$ are basically of order 1 and $\epsilon \ll 1$ denotes a small parameter. This number is often related to a bubble radius in practice. In the following and without restriction, we will simply take $\lambda(\mathbf{u}) = 1$ and $\theta(\mathbf{u}) = 1$.

As far as the interfacial quantities are concerned, we make the choice $u_I = u_2$ and $p_I = p_1$ which turns out to be mathematically consistent with both the linear degeneracy of the characteristic field associated with u_I , and the existence of an entropy-entropy flux pair. We do not enter the details and refer for instance the reader to [15]. Note however that other choices are possible.

The drift-flux model. The drift-flux model reads as follows :

$$\begin{cases} \partial_t \rho + \partial_x \rho u = 0 \\ \partial_t \rho Y + \partial_x (\rho Y u + \rho Y (1 - Y) u_r) = 0 \\ \partial_t \rho u + \partial_x (\rho u^2 + p + \rho Y (1 - Y) u_r^2) = \rho (1 - Y) f_1(\mathbf{v}) + \rho Y f_2(\mathbf{v}) \end{cases} \quad (19)$$

Here, the unknowns are the mixture density ρ , the mass fraction Y of one of the two phases (say for instance the phase 2) and the mixture velocity u . We set $\mathbf{v} = (\rho, \rho Y, \rho u)$.

The first equation is the classical mass conservation for the total density ρ . The partial density ρY is also conserved but we note that in addition to the usual transport term $\rho Y u$, the second equation involves an additional contribution $u_r = u_r(\mathbf{v})$ which represents an algebraic closure law defining the difference between the velocities of the two phases. This term is also present in the momentum equation. As already stated, the external forces $f_1(\mathbf{v})$ and $f_2(\mathbf{v})$ will be set to the gravity constant $-g$ in the following.

At last and in regards to the pressure term $p = p(\mathbf{v})$, we consider an isobaric closure law associated with two given barotropic pressures $p_1 = p_1(\rho_1)$ and $p_2 = p_2(\rho_2)$ for the two phases 1 and 2. More precisely, the following system is assumed to well-define the void fraction α_2 and the pressure p with respect to \mathbf{v} :

$$\begin{cases} p = p_2\left(\frac{\rho Y}{\alpha_2}\right) \\ p_1\left(\frac{\rho(1-Y)}{1-\alpha_2}\right) = p_2\left(\frac{\rho Y}{\alpha_2}\right) \end{cases}$$

Asymptotic analysis. As already said, our objective is to couple these models at a fixed interface. In order to propose a relevant numerical coupling strategy, we first studied in [7] how these models are related to each other and proved a hierarchy between the two-pressure and the drift-flux models. More precisely, we proved that the solutions of the drift-flux model correspond to the first-order equilibrium approximation of the solutions of the two-pressure model. The method of proof is based on an asymptotic analysis with respect to the small parameter ϵ using the Chapman-Enskog method, and the corresponding relative velocity u_r is given either by a Darcy-type differential closure law or an algebraic closure law in the spirit of

Zuber-Findlay models [22]. The main two steps of this analysis are briefly recalled here and we refer the reader to [7] for more details.

We are interested in the solutions of the two-pressure model near the equilibrium defined by

$$\begin{cases} p_r := p_1(\rho_1) - p_2(\rho_2) = 0, \\ u_r := u_2 - u_1 = 0. \end{cases}$$

Following the Chapman-Enskog method, these solutions are parametrized by ϵ and we assume that they satisfy the following first-order development in power series over the small parameter ϵ :

$$\begin{cases} p_r = 0 + \epsilon p_r^1 + \mathcal{O}(\epsilon^2), \\ u_r = 0 + \epsilon u_r^1 + \mathcal{O}(\epsilon^2). \end{cases} \tag{20}$$

Note that the dependance on ϵ is not explicit in order to avoid cumbersome notations. We are thus able to prove the following result.

Theorem 5.1. ([7]) *Let us define the mixture variables*

$$\begin{aligned} \rho &:= \alpha_1 \rho_1 + \alpha_2 \rho_2, \\ \rho u &:= \alpha_1 \rho_1 u_1 + \alpha_2 \rho_2 u_2, \\ \rho Y &:= \alpha_2 \rho_2, \end{aligned}$$

from the two-pressure model. Then, the first-order equilibrium system associated with the two-pressure model (18) reads exactly as the drift-flux model (19) with the following Darcy-type closure law for the relative velocity u_r :

$$|u_r| u_r = \epsilon^2 (\rho_2 - \rho_1) \alpha_1 \alpha_2 \frac{\partial_x p}{\rho} \tag{21}$$

In other words, the drift-flux model coincides with the reduced model in which the second (and higher) order terms in ϵ are neglected. The proof of this result simply consists in first inserting the Chapman-Enskog expansions (20) of u_r and p_r in the two-pressure model, and then keeping the first-order terms in ϵ while neglecting the higher-order terms.

Remark 3. It is important to notice that the Darcy-type closure law (21) still involves a second-order term in ϵ . This term has not been neglected in agreement with the classical form of the drift-flux models.

Remark 4. It is also important to mention that thanks to the second-order term ϵ^2 in the pressure relaxation coefficient of the two-pressure model, the first-order pressure correction p_r^1 turns out to be zero. As a consequence, the first-order equilibrium system does not depend on $\Theta(\mathbf{u})$.

The hydrodynamic closure law (21) is a Darcy-like law in the sense that u_r depends on \mathbf{v} but also on the first derivative $\partial_x p$. This is only the first step towards a classical drift-flux model. Our objective is now to get a classical drift-flux model with an algebraic (*i.e.* a zeroth-order) closure law.

To do so, we focus on the so-called permanent flows. Such flows are defined as the long-time limit of the solutions of the drift-flux model along the characteristics of the flow. We then write down the governing equation for the momentum in the

associated Lagrangian-like coordinates and neglecting the ϵ^2 and higher-order terms leads to the following classical equation :

$$D_t u + \frac{1}{\rho} \partial_x p = -g.$$

Since we aim at focusing on long-time limit solutions, it is natural to introduce the scaling $s = t\epsilon$ so as to get

$$\epsilon D_s u + \frac{1}{\rho} \partial_x p = -g.$$

Now letting ϵ go to 0 allows to recover the classical hydrostatic equilibrium relation

$$\partial_x p = -\rho g.$$

Such a balance between the gradient of the pressure p and the external forces is the key point in the derivation of a zeroth-order closure law for the relative velocity u_r . It is stated in the following theorem.

Theorem 5.2. ([7]) *Let us assume that the hydrostatic equilibrium*

$$\partial_x p = -\rho g \tag{22}$$

is satisfied. Then the first-order equilibrium system associated with the two-pressure model (18) reads exactly as the drift-flux model (19) with the following algebraic closure law for the relative velocity u_r :

$$|u_r| u_r = -\epsilon^2 (\rho_2 - \rho_1) \alpha_1 \alpha_2 g. \tag{23}$$

We have thus proved a hierarchy between the two-fluid two-pressure model and the drift-flux model using asymptotic mechanisms. In other words, the solutions of the two-fluid two-pressure model behave like the solutions of the drift-flux model with the algebraic closure law (23) when $\epsilon \rightarrow 0$ and at first order accuracy.

The numerical coupling procedure. Let us now consider the coupling problem at point $x = 0$ of the two-pressure model in the left part of the domain ($x < 0$) and the drift-flux model with closure relation (23) in the right part of the domain ($x > 0$). The proposed numerical scheme is taken from [14] and only the key points are given here. It is based again on a finite volume approach so that exactly the same notations as in Section 4 are used for the time and space steps and the mesh (cells and points). Regarding the piecewise constant approximate solutions, $\mathbf{u}_{j+1/2}^n$ for $j < 0$ will correspond to the two-pressure model and $\mathbf{v}_{j+1/2}^n$ for $j \geq 0$ will be associated with the drift-flux model.

The strategy is motivated by the asymptotic result we have just recalled and has already been used in other contexts, see for instance [9], [19] and the references therein. It is often called the father model technique. Here of course, the two-pressure model naturally plays the role of the father model. The strategy is made of two steps. In the first one, the two-pressure model is numerically solved on the whole domain, *i.e.* including the cells $\mathcal{C}_{j+1/2}$ for $j \geq 0$. This step relies on a relevant reconstruction strategy. In the second one, a simple projection procedure is applied on the cells $\mathcal{C}_{j+1/2}$ for $j \geq 0$ in order to get back an approximate solution consistent with the drift-flux model. Proceeding this (natural) way, the proposed numerical scheme for the drift-flux model is expected to asymptotically comply with the one associated with the two-pressure model. Let us now give this more details.

First step : $t^n \rightarrow t^{n+1-}$. In order to solve the two-pressure model in the whole domain, we first propose to define an approximate solution of this model in the right part of the domain by lifting $\mathbf{v}_{j+1/2}^n$, $j \geq 0$. It thus amounts to define \mathbf{u} from \mathbf{v} and this procedure is expected to be consistant with the drift law defining u_r . We proceed as follows for all $j \geq 0$. The mass fractions are first defined setting :

$$\begin{aligned} (\alpha_2 \rho_2)_{j+1/2}^n &= (\rho Y)_{j+1/2}^n \\ (\alpha_1 \rho_1)_{j+1/2}^n &= \rho_{j+1/2}^n - (\alpha_2 \rho_2)_{j+1/2}^n. \end{aligned}$$

Then, $(\alpha_1)_{j+1/2}^n$ and $(\alpha_2)_{j+1/2}^n = 1 - (\alpha_1)_{j+1/2}^n$ are defined thanks to the isobaric relation

$$p_1 \left(\frac{(\alpha_1 \rho_1)_{j+1/2}^n}{(\alpha_1)_{j+1/2}^n} \right) = p_2 \left(\frac{(\alpha_2 \rho_2)_{j+1/2}^n}{(\alpha_2)_{j+1/2}^n} \right).$$

At last, we seek the momentum $(\alpha_1 \rho_1 u_1)_{j+1/2}^n$ and $(\alpha_2 \rho_2 u_2)_{j+1/2}^n$ as the solutions of the following 2×2 nonlinear system involving the drift law :

$$\begin{cases} (\rho u)_{j+1/2}^n = (\alpha_1 \rho_1 u_1)_{j+1/2}^n + (\alpha_2 \rho_2 u_2)_{j+1/2}^n \\ |(u_r)_{j+1/2}^n| (u_r)_{j+1/2}^n = -\epsilon^2 ((\rho_2)_{j+1/2}^n - (\rho_1)_{j+1/2}^n) (\alpha_1)_{j+1/2}^n (\alpha_2)_{j+1/2}^n g, \end{cases}$$

where of course $\rho_k = (\alpha_k \rho_k) / \alpha_k$ and $u_k = (\alpha_k \rho_k u_k) / (\alpha_k \rho_k)$ for each $k = 1, 2$, and $u_r = u_2 - u_1$. Note that the topology of the flow under consideration is expected to ensure existence and uniqueness of a solution to this system. In other words, the sign of the relative velocity u_r and then the value of $|u_r|$ is assumed to be defined without ambiguity.

Equipped with this piecewise constant approximation of \mathbf{u} in the whole domain, we are now in position to numerically solve the two-pressure model in the time interval $[t^n, t^{n+1}]$. This leads to an updated sequence of approximate values $\mathbf{u}_{j+1/2}^{n+1-}$, $\forall j$.

Step 2 : $t^{n+1-} \rightarrow t^{n+1}$. The aim of this step is to recover a consistant approximation of the drift-flux model in the right part of the domain. With this in mind, we propose to keep unchanged the updated values in the left part, setting

$$\mathbf{u}_{j+1/2}^{n+1} = \mathbf{u}_{j+1/2}^{n+1-}, \quad \forall j < 0,$$

and to simply project it in the right part. More precisely, $\mathbf{v}_{j+1/2}^{n+1}$ for $j \geq 0$ is defined by the following natural relations :

$$\begin{aligned} (\rho Y)_{j+1/2}^{n+1} &= (\alpha_2 \rho_2)_{j+1/2}^{n+1-} \\ \rho_{j+1/2}^{n+1} &= (\alpha_1 \rho_1)_{j+1/2}^{n+1-} + (\alpha_2 \rho_2)_{j+1/2}^{n+1-} \end{aligned}$$

and

$$(\rho u)_{j+1/2}^{n+1} = (\alpha_1 \rho_1 u_1)_{j+1/2}^{n+1-} + (\alpha_2 \rho_2 u_2)_{j+1/2}^{n+1-}$$

This solution is thus expected to approach the solution of the drift-flux model up to second or higher order terms in ϵ .

The numerical scheme we used to define $\mathbf{u}_{j+1/2}^{n+1-}$ is based on a relaxation approximation of the two-pressure model, including both the convective part of the model and its velocity relaxation term. The latter thus received an upwind treatment. On the contrary, the other sources such as the pressure relaxation term are taken into account using classical centered approximations. Such a strategy is motivated by the now well-known well-balanced and asymptotic preserving properties, see for instance [12] and the numerous references therein. For the full description of the

algorithm, we refer the reader to [14] (note that the paper [8] is submitted on this subject, including an extension to the non barotropic case).

Remark 5. Note that such a coupling procedure is by construction conservative with respect to the partial mass $\alpha_1\rho_1$, $\alpha_2\rho_2$ and total momentum $\rho u = \alpha_1\rho_1u_1 + \alpha_2\rho_2u_2$. Note also that it is relevant provided that ϵ is small and the flow almost satisfies the hydrostatic equilibrium relation. This is indeed necessary for the approximate solution to realize a good approximation of the drift-flux solution in the right part of the domain.

Numerical illustration. In order to assess the validity of our coupling approach and to numerically illustrate the proximity result of the solutions of the two-pressure and drift-flux models, we consider an ascending dispersed two-phase flow in a vertical bubbly column of 1m length. The bottom is located at $x = -0.5$, the top at $x = 0.5$ and the coupling interface at $x = 0$.

The pressure laws are given by stiffened gas equations of states

$$p_k(\rho_k) = A_k(\gamma_k - 1)\rho_k^{\gamma_k} - P_{k,\infty}$$

where the coefficients are taken to be

$$\begin{cases} \gamma_1 = 4.1, \gamma_2 = 1.4 \\ P_{1,\infty} = 900 \cdot 10^5 Pa, P_{2,\infty} = 0, \\ A_1 = 1.346 \cdot 10^{-4}, A_2 = 62268. \end{cases}$$

These values are such that when $p_1 = p_2 = 150 \text{ bar}$ and $T_1 = T_2 = 342.16 \text{ }^\circ C$, the densities ρ_1 and ρ_2 correspond respectively to the saturation values of the liquid and vapor water densities, namely $\rho_1 = 603.52 \text{ kg/m}^3$ and $\rho_2 = 96.727 \text{ kg/m}^3$.

Theoretical boundary conditions are such that at the entrance we impose a non zero relative velocity such that $u_1 = 5 \text{ m/s}$ and $u_2 = 15 \text{ m/s}$, the void fraction $\alpha_1 = 0.97$, and the mixture pressure $p = 155 \cdot 10^5 Pa$. At the exit, we only impose the mixture pressure $p = 150 \cdot 10^5 Pa$.

From a numerical point of view, fictitious states were used with Dirichlet boundary conditions at the entrance (with $p_1 = p_2$) and half-Riemann problems in the sense of Dubois and LeFloch [13] at the exit.

In such a configuration, an equilibrium is expected to take place in very long time between the pressure gradient and the gravity terms. so that we expect a proximity between the solutions of the two models under consideration. We then plot on the next picture the stationary profiles of the relative velocity given by a 100-point mesh and with different methods. More precisely, we propose to compare the solutions given by the coupling procedure we described above, and by the two-pressure model and the drift-flux model respectively considered in the whole domain (the above strategy is obviously adapted to the these extreme situations). Different values of ϵ are considered.

As expected we observe that the more ϵ is small, the best is the agreement between the three curves in the stationary regime and the shorter is the distance associated with the transitory regime.

This test case shows a typical situation of physically relevant coupling problem. It is indeed theoretically justified by a link between both models (asymptotic analysis) to be coupled, it is numerically relevant since the coupling procedure is natural and conservative with respect to the partial mass and total momentum, and importantly we obtain similar results between a simulation performed with the two-pressure

model only (expensive) and the coupling (less expensive) so that a significant gain may be obtained in practice.

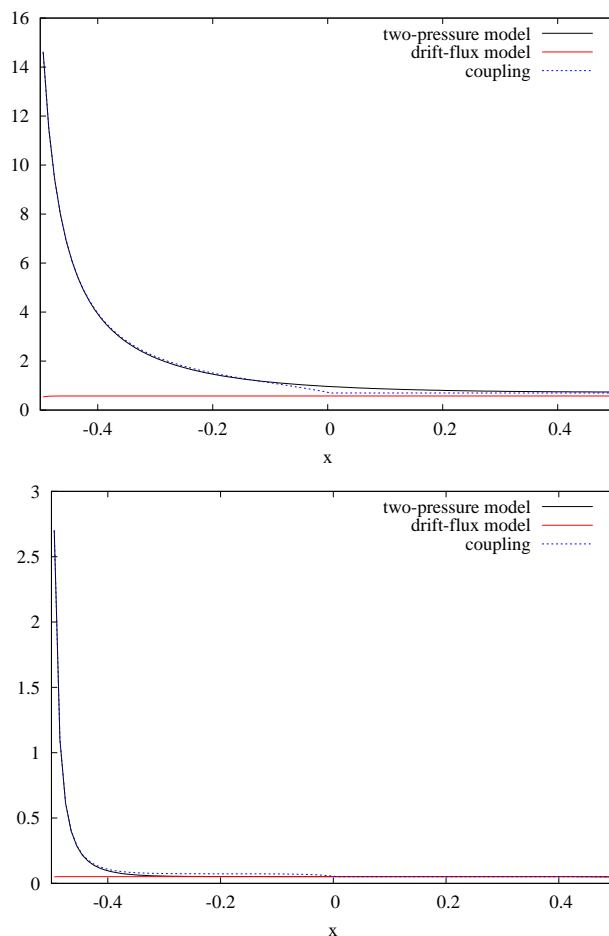


FIGURE 11. $\epsilon^2 = 10^{-1}$ (Top) and $\epsilon^2 = 10^{-3}$ (Bottom)

6. Conclusion. This paper presents an introduction to the coupling of hyperbolic models from both a theoretical and industrial point of view. It reviews in particular some of the results obtained by a working group between the J.-L. Lions Laboratory (University P. et M. Curie Paris 6) and the CEA-Saclay. It consists of two independent parts. The first part considers the coupling of two scalar conservation equations and the second part is devoted to the coupling of two barotropic two-phase flow models.

REFERENCES

- [1] A. Ambroso, C. Chalons, F. Coquel, E. Godlewski, F. Lagoutière, P.-A. Raviart and N. Seguin, *Coupling of multiphase flow models*, Proceedings for the Eleventh International Meeting on Nuclear Thermal-Hydraulics (NURETH), 2005.

- [2] A. Ambroso, C. Chalons, F. Coquel, E. Godlewski, F. Lagoutière, P.-A. Raviart and N. Seguin, *Homogeneous models with phase transition: Coupling by finite volume methods*, Finite volumes for complex applications, IV (Marrakech 2005) 483–492, Hermes Science, 2005.
- [3] A. Ambroso, C. Chalons, F. Coquel, E. Godlewski, F. Lagoutière, P.-A. Raviart and N. Seguin, *The coupling of homogeneous models for two-phase flows*, Int. Journal for Finite Volume, **4**, 2007. <http://www.latp.univ-mrs.fr/IJFV/>.
- [4] A. Ambroso, C. Chalons, F. Coquel, E. Godlewski, F. Lagoutière, P.-A. Raviart and N. Seguin, *A relaxation method for the coupling of systems of conservation laws*, Hyp2006 Proceedings. Springer: Berlin, 2007.
- [5] A. Ambroso, C. Chalons, F. Coquel, E. Godlewski, F. Lagoutière, P.-A. Raviart and N. Seguin, *Coupling of general Lagrangian systems*, Mathematics of Computation, **77** (2008), 909–941.
- [6] A. Ambroso, C. Chalons, F. Coquel, E. Godlewski, F. Lagoutière, P.-A. Raviart and N. Seguin, *Relaxation methods and coupling procedure*, International Journal for Numerical Methods in Fluids, **56** (2008), 1123–1129.
- [7] A. Ambroso, C. Chalons, F. Coquel, T. Galié, E. Godlewski, P.-A. Raviart and N. Seguin, *The drift-flux asymptotic limit of barotropic two-phase two-pressure models*, Comm. Math. Sci., **6** (2008), 521–529.
- [8] A. Ambroso, C. Chalons and P.-A. Raviart, *A Godunov-type method for the seven-equation model of compressible two-phase flow*, submitted (2010).
- [9] A. Ambroso, J.-M. Hérard and O. Huriisse, *A method to couple HEM and HRM two-phase flow models*, Computers and Fluids, **38** (2009), 738–756.
- [10] B. Boutin, C. Chalons and P.-A. Raviart, *Existence result for the coupling of two scalar conservation laws with Riemann initial data*, to appear in M3AS, (2010).
- [11] C. Chalons, P.-A. Raviart and N. Seguin, *The interface coupling of the gas dynamics equations*, Quarterly of Applied Mathematics, **66** (2008), 659–705.
- [12] C. Chalons, F. Coquel, E. Godlewski, P.-A. Raviart and N. Seguin, *Godunov-type schemes for hyperbolic systems with parameter dependent source. The case of Euler system with friction*, Internal Report R09039, Laboratoire J.-L. Lions, <http://www.ann.jussieu.fr>, to appear in M3AS, (2010).
- [13] F. Dubois and P.-G. LeFloch, *Boundary conditions for nonlinear hyperbolic systems of conservation laws*, J. Differential Equations, **71** (1988), 93–122.
- [14] T. Galié, “Couplage Interfacial de Modèles en Dynamique des Fluides. Application aux Écoulements Diphasiques,” PhD thesis, Université Pierre et Marie Curie - Paris 6, France, (2009).
- [15] T. Gallouët, J.-M. Hérard and N. Seguin, *Numerical modeling of two-phase flows using the two-fluid two-pressure approach*, Mathematical Models and Methods in Applied Sciences (M3AS), **14** (2004), 663–700.
- [16] E. Godlewski and P.-A. Raviart, *The numerical interface coupling of nonlinear hyperbolic systems of conservation laws. I. The scalar case*, Numer. Math., **97** (2004), 81–130.
- [17] E. Godlewski, K.-C. Le Thanh and P.-A. Raviart, *The numerical interface coupling of nonlinear hyperbolic systems of conservation laws. II. The case of systems*, M2AN Math. Model. Numer. Anal., **39** (2005), 649–692.
- [18] A. Guelfi, D. Bestion, M. Boucker, P. Boudier, P. Fillion, M. Grandotto, J.-M. Hérard, E. Hervieu and P. Péturaud, *NEPTUNE: A new software platform for advanced nuclear thermal hydraulic*, Nuclear Science and Engineering, **156** (2007), 281–324.
- [19] J.-M. Hérard and O. Huriisse, *Some attempts to couple distinct fluid models*, Network and Heterogeneous Media, submitted.
- [20] O. Huriisse, “Techniques de Couplages de Modèles Hyperboliques en Thermohydraulique Diphasique,” PhD thesis, Université de Provence, France, 2006.
- [21] C. Lattanzio and D. Serre, *Convergence of a relaxation scheme for hyperbolic systems of conservation laws*, Numer. Math., **88** (2001), 121–134.
- [22] N. Zuber and J.-A. Findlay, *Average volumetric concentration in two-phase flow systems*, J. Heat. Transfer., **68** (1965), 453–468.

Received January 2010; revised April 2010.

E-mail address: chalons@math.jussieu.fr